Synthesis, Characterization and Adsorption Properties of the New Chitosan/Natural Zeolite Composite for the Nitrate Removal from Aqueous Solution

Toktam Shenavaei Zare[1] * iD, Zahra-Beagom Mokhtari-Hosseini[2] iD

1. Department of Chemical Engineering, Faculty of Petroleum and Petrochemical Engineering, Hakim Sabzevari University, Sabzevar, Iran. E-mail: t.shnavaei@hsu.ac.ir
2. Department of Chemical Engineering, Faculty of Petroleum and Petrochemical Engineering, Hakim Sabzevari University, Sabzevar, Iran. E-mail: z.mokhtari@hsu.ac.ir

ARTICLE INFO	ABSTRACT
	High concentrations of nitrates in water can have several effects on human and aquatic health, therefore, control levels of nitrates are essential. In this work, the adsorption of nitrate on beads of chitosan and zeolite composites was investigated. According to Transmission Electron Microscopy results, the employed zeolite has clinoptilolite and calcite with 50-870 nm particle size. The association between chitosan and zeolite was also verified by chemical and morphological characterizations. Results showed chitosan/acid-modified natural zeolite composite beads (Ch/AMZ) exhibited higher nitrate adsorption than other ones. The nitrate adsorption on Ch/AMZ as a function of pH, contact time, and bead concentration was optimized by a response surface method using batch experiments. According to the results, at the computed optimum operating conditions the maximum nitrate removal efficiency, 98.2% with Ch/AMZ, and adsorption capacity, 22.48 mg g^{-1} were obtained. The presented nitrate removal technique with the proposed eco-friendly adsorbent can be considered a critical approach for removing nitrate from drinking water and possibly using it on an industrial scale as a green and economical method for water and wastewater treatment.

Introduction

Due to the increasing world population and the growing need for water, the exploitation of groundwater resources and saline water has been necessary in recent decades [1, 2]. Since high nitrate concentration in drinking water can harm health, especially for fetuses and infants, nitrate removal from groundwater resources is one of the essential needs in rural and some urban areas [3].

Technologies that are being used for the removal of nitrate include reverse osmosis [4], electrodialysis [5, 6], ion exchange [7, 8] and adsorption [9]. Among several technologies applied for nitrate removal, adsorption by sorbents (synthetic, bio, and mineral sorbents) is one of the most effective because the technique uses equipment that is easily accessible, not energy-consuming, straightforward, and inexpensive [9-12]. Activated carbon [13, 14], Red mud [15], agriculture wastes [16-18], and biopolymers [11, 19, 20] were used to remove nitrate.

---

* Corresponding Author: T. Shenavaei Zare (E-mail address: t.shnavaei@hsu.ac.ir)

Chitosan is a low-cost biopolymer that is found in the exoskeleton of crustaceans like crabs [21]. Reportedly, several studies focused on chitosan as an adsorbent because of its non-toxicity and biodegradability [9]. The chitosan amine and hydroxyl groups make it a promising material for nitrate sorption [22]. Using chitosan hydrogel beads is a method for obtaining nitrate from aqueous solutions [22-25]. However, chitosan dissolves easily in acidic wastewater, and its mechanical properties are weak, which limits its application in wastewater treatment. Because of physical and chemical interactions between inorganic and organic components, chitosan's mechanical properties can be enhanced when it is combined with inorganic components [26], such as bentonite [27, 28], montmorillonite [29, 30], silica [31, 32], activated clay [33, 34], alumina [35], perlite [36], and zeolite [37-43].

Zeolites have also received more attention due to their many advantages such as easy access, low cost, easy separation, recyclability, and reuse. Actually, due to the strong mechanical stability of zeolites, the chitosan's mechanical strength and adsorption performance regarding different pollutants can be enhanced by synthesizing composites of chitosan/zeolite [37-44].

The novelty of the present study is that low-cost composite beads comprising the chitosan and modified Sabzevar zeolite were used as adsorbent in nitrate removal processes for the first time and optimal conditions were determined by response surface methodology (RSM).

Materials and Methods

Materials

Chitosan with 99.95% purity and Hexadecyltrimethyl ammonium bromide (HDTMA-Br) were purchased from Sigma Company. The natural zeolite was prepared from a mineral deposit in Chah-e Talkh village in Sabzevar town, North East of Iran.

Zeolite-Modification

For the first, zeolite rock was crushed by a ball mill for 3 h at 500 rpm and then zeolite powder was washed with distilled water and dried, zeolite powder was stored in the desiccators for the next stages. The zeolite powder (Z) was activated by soaking into hydrochloric acids according to the following condition: 10 g of zeolite powder and 500 mL of HCl solution (1 N) were stirred at 150 rpm and 60 °C for 24 h. Then the prepared mixture was centrifuged, and the solid powder was washed with distilled water to attain a neutral pH. The absence of Cl^- in the solid powder was confirmed by $AgNO_3$ solution 0.1 mol/dm^3. The sample was dried in an oven at 60 °C overnight [45]. The prepared acid-modified natural zeolite is named AMZ. 10 g of zeolite powder and 100 mL of HDTMA-Br solution at the concentration of 30 mmol /L were stirred at 150 rpm and 30°C for 24 h. Then centrifuged, the solid residue was rinsed with distilled water two times and dried at 60 °C overnight [46, 47]. The surfactant-modified natural zeolite is named SMZ.

Chitosan/Zeolite Composite Beads Synthesis

One gram of chitosan was added to 30 ml of 5% acetic acid solution to prepare the chitosan solution. Then, this solution of chitosan and acetic acid was stirred by using a magnetic stirrer at 200 rpm for 4 hr to ensure complete dissolution of chitosan. The solution was injected into a 500 mL flask containing NaOH (0.50 M) using a syringe pump equipped with a needle with 0.337 mm inner diameter and stirred at 150 rpm for 3 h to prepare the chitosan beads. The size of the beads was controlled using an air compressor that injects high-velocity air (9.6 m/s) into

the needle head (Fig. 1). The beads formed were left for 30 minutes for proper formation of the beads, then filtered and washed several times with deionized water to reach a neutral pH.
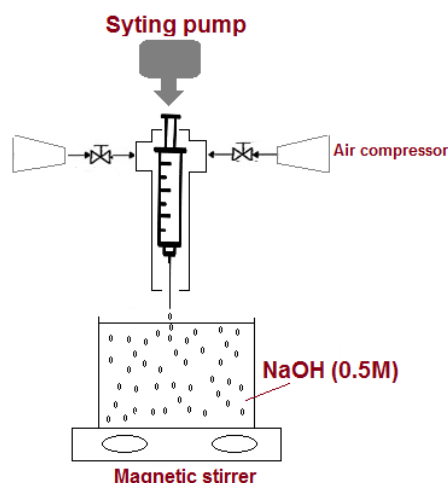

Fig. 1. Experimental set-up for production of chitosan/zeolite beads

To prepare chitosan/zeolite composite beads, 2.0 g chitosan was added to 60 ml of 5% acetic acid solution. After chitosan and acetic acid were mixed by a magnetic stirrer, 1.0 g zeolites (Z, AMZ, or SMZ) were added into this solution and stirred by using a magnetic stirrer at 200 rpm for 4 hr to ensure complete dissolution of chitosan. The composite beads suspension was injected into a 500 Ml flask containing NaOH (0.50 M), based on the method presented in the previous paragraph. The prepared chitosan/zeolite composite beads are named Ch/Z, Ch/AMZ, and Ch/SMZ.

Natural Zeolite, Chitosan, and Chitosan/Zeolite Composite Beads Characterization

Natural zeolite was rinsed with distilled water and crushed by a ball mill for 3 h at 500 rpm then, the prepared zeolite powder was dried at 60°C for 24 h. To identify and describe the composition, structure, elemental analysis, and percentage of minerals of the Sabzevar natural zeolite, transmission electron microscopy (TEM) (CM120, Philips), X-ray fluorescence (XRF) (CE3021, CECIL Instruments) and X-ray diffraction (XRD) (X' Pert PW 3040/60, Philips) were used. The functional groups present in the chitosan, Sabzevar natural zeolite, surfactant, Ch/Z, Ch/AMZ, and Ch/SMZ in the dried state were also recorded by a Fourier transform infrared spectroscopy (FTIR) (Shimadzu, Japan). The Brunauer-Emmett-Teller (BET) method was used to determine the surface area and total pore volume for each composite bead by BET instrument (BELSORP mini II, BEL). Field emission scanning electron microscopy (FESEM) (MIRA III, TESCAN, Czech Republic) was used to study the size and morphology of composite beads.

To measure the solubility of the beads in different acid solutions, 1.0 g of beads was put in 50 mL flasks containing various types of acid solutions (0.1 and 1.0 N HCl and 5% acetic acid) and were shaken at 150 rpm at 25°C for 24 h. A vacuum filtration technique was used to separate beads from the solution and the weight of the remaining beads was measured. The beads were considered soluble when the weight loss was greater than 5%.

Selection of the "Best" Beads

In the first stage of adsorption experiments, four types of beads (Ch, Ch/Z, Ch/AMZ, and Ch/SMZ) were used in similar operating conditions (50 mg/L nitrate-nitrogen (NO_3-N), 12 g/L beads concentration, 1h contact time, 25 °C, 150 rpm, and pH = 7). After the adsorption process, the adsorbent particles were separated from the suspensions by filtration, and the residual concentration of NO_3-N was determined using the UV-Vis spectrophotometer at 220 nm. To

decrease the experimental errors, all tests were conducted three times, and the mean experimental data was reported.

Response surface method (RSM)

The purpose the nitrate adsorption optimization is to maximize removal efficiency. The nitrate adsorption process depends on different variables. Therefore, a large number of experiments should be performed. Using an experimental design, the number of experiments is reduced In this research, RSM was utilized to explore the effect of effective variables [45, 48]. According to the preliminary adsorption experiments, it was found that the pH, contact time, and the dose of adsorbent are the most important independent variables on the nitrate adsorption from aqueous solution. Levels of variables were selected based on primary studies and have been shown in Table 1. Experimental design and data analysis was conducted using Design Expert. The independent variables for the nitrate adsorption process (initial concentration 50 mg/L NO_3-N) were optimized. Central composite design (CCD) was employed to optimize variables and predict the best value of the response using the Design Expert software version 7.0.

Table 1. The levels of the affective variables for nitrate removal from aqueous solution

Variables	Variable Code	Coded Value				
		(-1.683)	(-1)	(0)	(+1)	(+1.683)
pH	A	3.64	5	7	9	10.36
Contact time (min)	B	19.55	40	70	100	120.45
Bead concentration (g/L)	C	1.32	2	3	4	4.68

Adsorption Isotherms

The adsorption isotherm experiments were conducted to evaluate removal efficiencies and maximum adsorption capacities. To investigate the adsorption isotherms, a series of bottles containing nitrate solutions with different NO_3-N concentrations (C_o) between 10-200 mg/L and Ch/AMZ with 5.5 g/L concentration was kept at 25°C, 150 rpm, and pH = 6 until the equilibrium concentration is maintained. The agreement of experimental values with different adsorption isotherms was examined. The concentrations of the nitrate in the adsorbent phase at equilibrium were determined according to the following equation:

$$q_e = \frac{(C_0 - C_e) \times V}{M}$$

(1)

In Eq. 1; q_e (mg/g) is the concentration of the nitrate in the adsorbent phase at equilibrium (mg/g), and C_o and C_e (mg/L) are the initial and equilibrium NO_3-N concentration. V (L) is the volume of aqueous solution, and M (g) is the adsorbent mass [49].

Results and Discussions

Natural Zeolite, Chitosan, and Chitosan/Zeolite Composite Beads Characterization

According to the XRF results in Table 2, the mass ratio of SiO_2/Al_2O_3 in the natural zeolite is equal to 6.55 and 15.62% of loss on ignition (L.O.I.) indicating the percentage of volatile components, mainly crystal-bound water and organic carbon (as CO_2). XRD results show the sabzevar zeolite has 76% clinoptilolite and 24% calcite. According to the TEM images in Fig. 2, the range of particle size of sabzevar zeolite was from 50 to 900 nm. The solubility of the

various beads in acid solution is presented in Table 3. As can be seen, the addition of zeolite to chitosan reduces the solubility of chitosan in acidic solutions, so the produced composite beads are more stable than chitosan beads in the treatment of acidic effluents. The average diameter of wet non-spherical chitosan and chitosan/zeolite beads were 0.500 ± 0.080 and 0.550 ± 0.085 mm respectively.
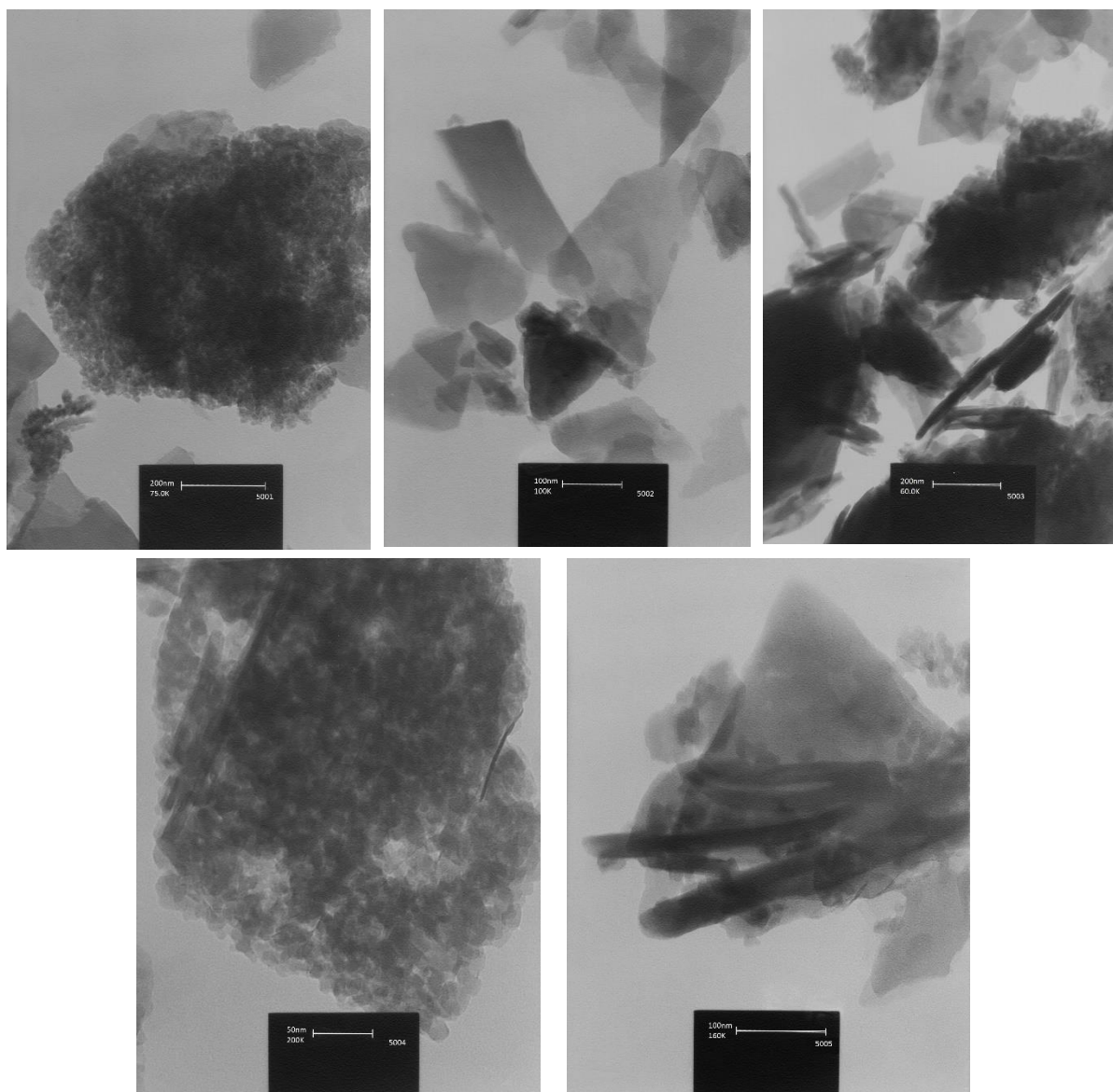
Fig. 2. TEM micrographs natural Sabzevar zeolite powder with different magnification

Table 2. The XRF results of the natural zeolite

Elements	SiO_2	Al_2O_3	Na_2O	MgO	CaO	K_2O	TiO_2	MnO	P_2O_5	Fe_2O_3	SO_3	LOI
Perception	62.68	9.57	2.43	0.77	5.51	1.76	0.17	0.09	0.03	0.041	0.00	15.62

Table 3. Solubility of the various beads in various acid solutions

Acid solution	Ch	Ch-Z	Ch-AMZ	Ch-SMZ
1.0 N HCl	Soluble	Soluble	Soluble	Soluble
0.1 N HCl	Soluble	Insoluble	Insoluble	Soluble
5% acetic acid	Soluble	Insoluble	Insoluble	Insoluble

According to the BET results in Table 4, The specific surface area of the natural zeolite (Z) increased after acid treatment from 22.52 to 41.74 m²/g. The greatest pore volume belonged to

the AMZ with 0.1194 cm^3/g. The surface area and the total pore volumes of SMZ were 16.92 m^2/g and 0.0513 cm^3/g. The smaller surface area of SMZ compared with sabzevar zeolite represented the aggregation of the surfactant molecules on natural zeolite. The BET result shows that the surface area of Ch, Ch/Z, Ch/AMZ, and Ch/SMZ beads were found to be 18.92, 20.08, 38.04, and 15.72 m^2/g, respectively. The increase in the BET surface area of composite beads (Ch/Z, Ch/AMZ, and Ch/SMZ) than chitosan beads may be attributed to the incorporation of the more functional group.

Table 4. The BET results of the various zeolite and beads

Beads	Surface Area (m^2/g)	Total Pore Volume (cm^3/g)
Z	22.52	0.0807
AMZ	41.74	0.1194
SMZ	16.92	0.0513
Ch	18.92	0.0612
Ch/Z	20.08	0.0845
Ch/AMZ	38.04	0.9581
Ch/SMZ	15.72	0.0501

According to the FTIR spectrum of zeolite (Fig. 3), the peaks of the broad 3471 and 1629 cm^{-1} correspond to the vibration of water associated with K and Na in the channels and cavities of sabzevar zeolite 1066, 669-678, 555 and 461 cm^{-1} bands correspond to Si-O stretching, Al-O-Si, Al-O and Si-O-Si bending vibrations in zeolite, respectively. The peaks of the broad 2354 cm^{-1} correspond to the CO_2 molecules in the atmosphere. The peak at 3431 cm^{-1} in the FTIR spectrum of chitosan (Fig. 3) corresponds to stretching vibrations of the hydroxyl group. The vibration band at 2889, 1425, and 1350 cm^{-1} in the FTIR spectrum of chitosan are due to the C-H stretching vibrations and those at 1155 cm^{-1} and 1081 cm^{-1} are due to asymmetry C-O-C stretching vibrations of CH-O-CH and C-O stretching vibration of the CH-OH, respectively. Three characteristics of adsorption bands observed in chitosan at 3400, 1652, and 1323 cm^{-1}, as in the given order are due to the N-H, amid I, and amid III groups.

Si-O stretching vibration, Al-O-Si, Al-O, and Si-O-Si bending vibrations in zeolite have shifted to 1064, 547, 676-692, and 464 cm^{-1} in Ch/Z (Fig. 3). The peak at 719 cm^{-1} represents the stretching vibration of Si-C; this peak indicated bonding between chitosan and zeolite. The peaks of the N-H, amid I, and amid III groups present in Ch/Z have shifted to 3400, 1650, and 1338 cm^{-1}. The peaks of the broad 1631, 1334, 1051, and 790 cm^{-1} in FTIR spectrums of the AMZ correspond to Al-H, Al-OH or Al-OH2, Si-O, and Si-O-Si or Al-O-Al, respectively. Compared with the unmodified zeolite, bands of the AMZ at 1629 and 1334 cm^{-1} decreased sharply and the bands at 1051 and 790 cm^{-1} increased slightly. These are the powerful evidence for the dealumination process. For Ch/AMZ (Spectrum in Fig. 3) the bands corresponding to the Al-H, Al-OH or Al-OH2, Si-O have shifted to 1652, 1029, and 1041 cm^{-1}. The peaks of N-H, amid I, and amid III groups in chitosan have shifted to wave numbers centered at 3425, 1652, and 1298 for Ch/AMZ.

The peaks of the broad 2850, and 2918 cm^{-1} correspond to C-H stretches vibration modes of the methylene groups in surfactant (Fig. 3). The surfactant-modified zeolite, in contrast to unmodified zeolites, has new bands at 2923 and 2856 cm^{-1}, attributed to the antisymmetric CH2 and symmetric CH2, C-H stretching vibration modes of the methylene groups, respectively, which suggests that the surface of the natural zeolite is covered by the alkyl ammonium bromides. For Ch/SMZ, the bands corresponded to the antisymmetric CH2 and symmetric CH2, C-H stretching vibration modes of the methylene groups in SMZ have bands at 2923 and 2858 cm-1 and the N-H, amid I, and amid III groups present in chitosan peaks have shifted to wave numbers centered at 1303, 1650, 3413 cm^{-1}. The FTIR spectrum of Ch/Z and Ch/AMZ showed

a broad band around 3500-3100 cm^{-1}, showing enhanced hydrogen bonding. The absence of these bonds in the FTIR spectra of Ch/SMZ showed the formation of an electrostatic bond.

According to the results of FE-SEM in Fig. 4, chitosan particles are observed on the surface of Ch/Z, Ch/SMZ, and Ch/AMZ. According to the element mapping results (Fig. 5), the zeolite was dispersed homogeneously in Ch/Z, Ch/SMZ, and Ch/AMZ samples.
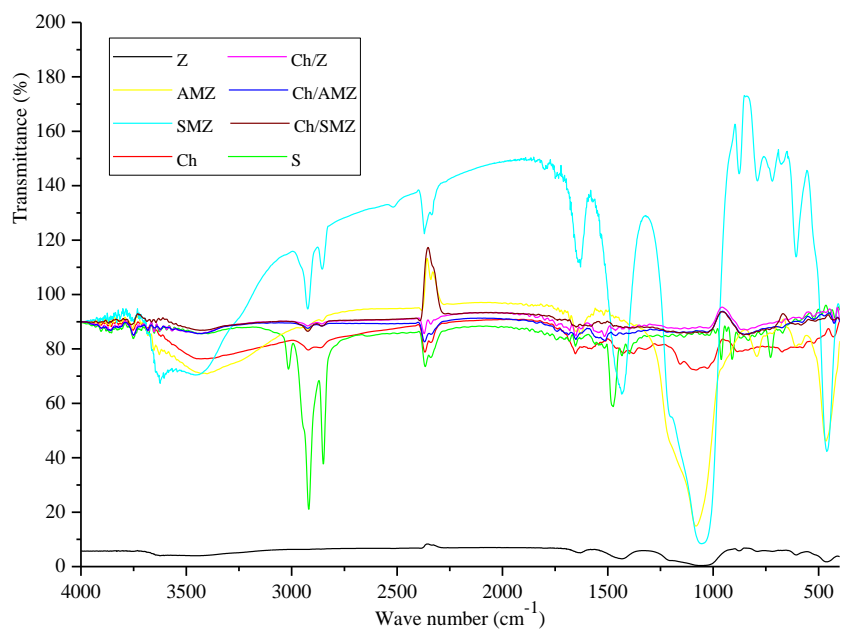

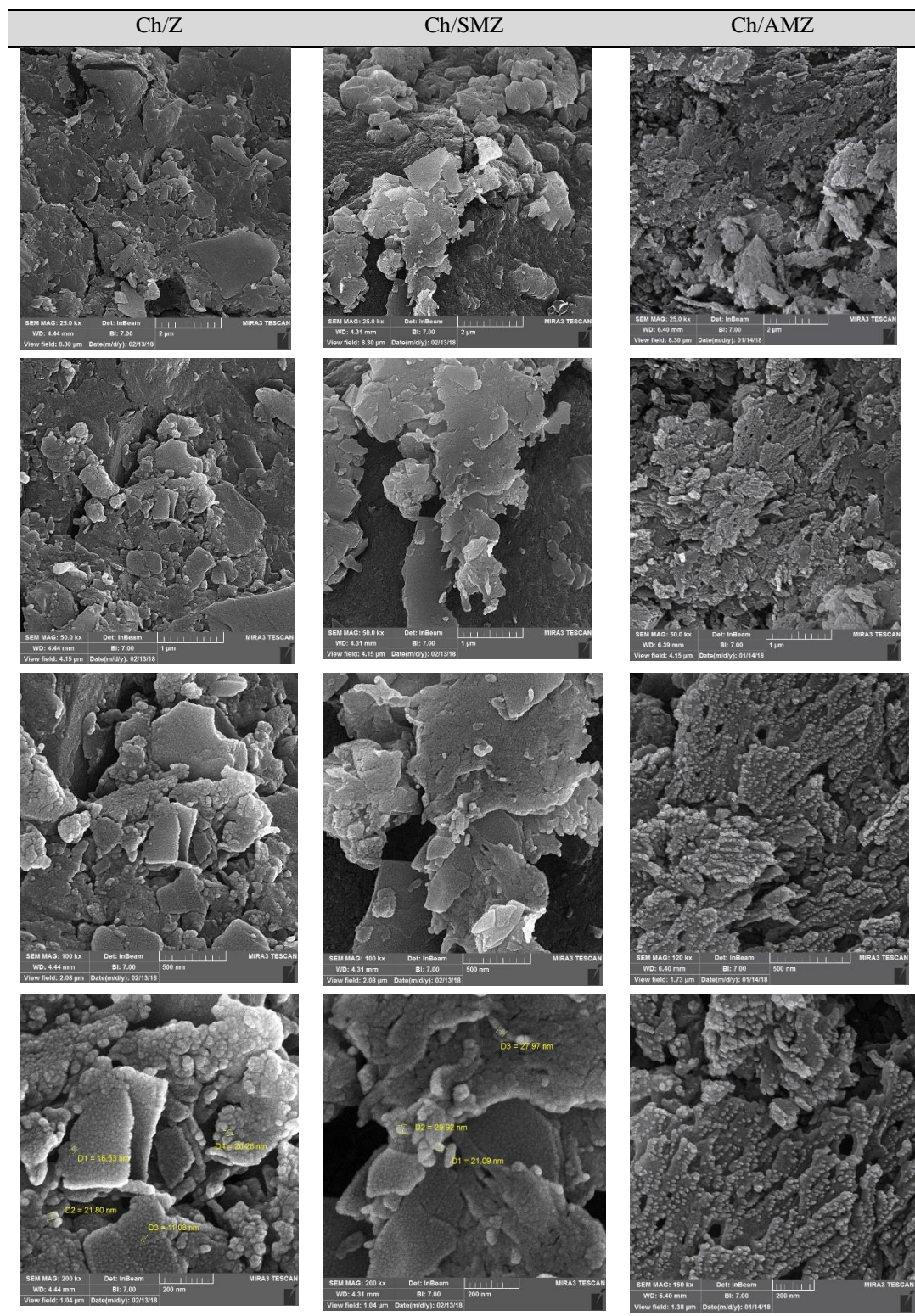**Fig. 3**. FTIR spectra of natural zeolite, chitosan, Ch/ Z, AMZ, SMZ, Ch/AMZ and Ch/ SMZ

Ch/Z	Ch/SMZ	Ch/AMZ

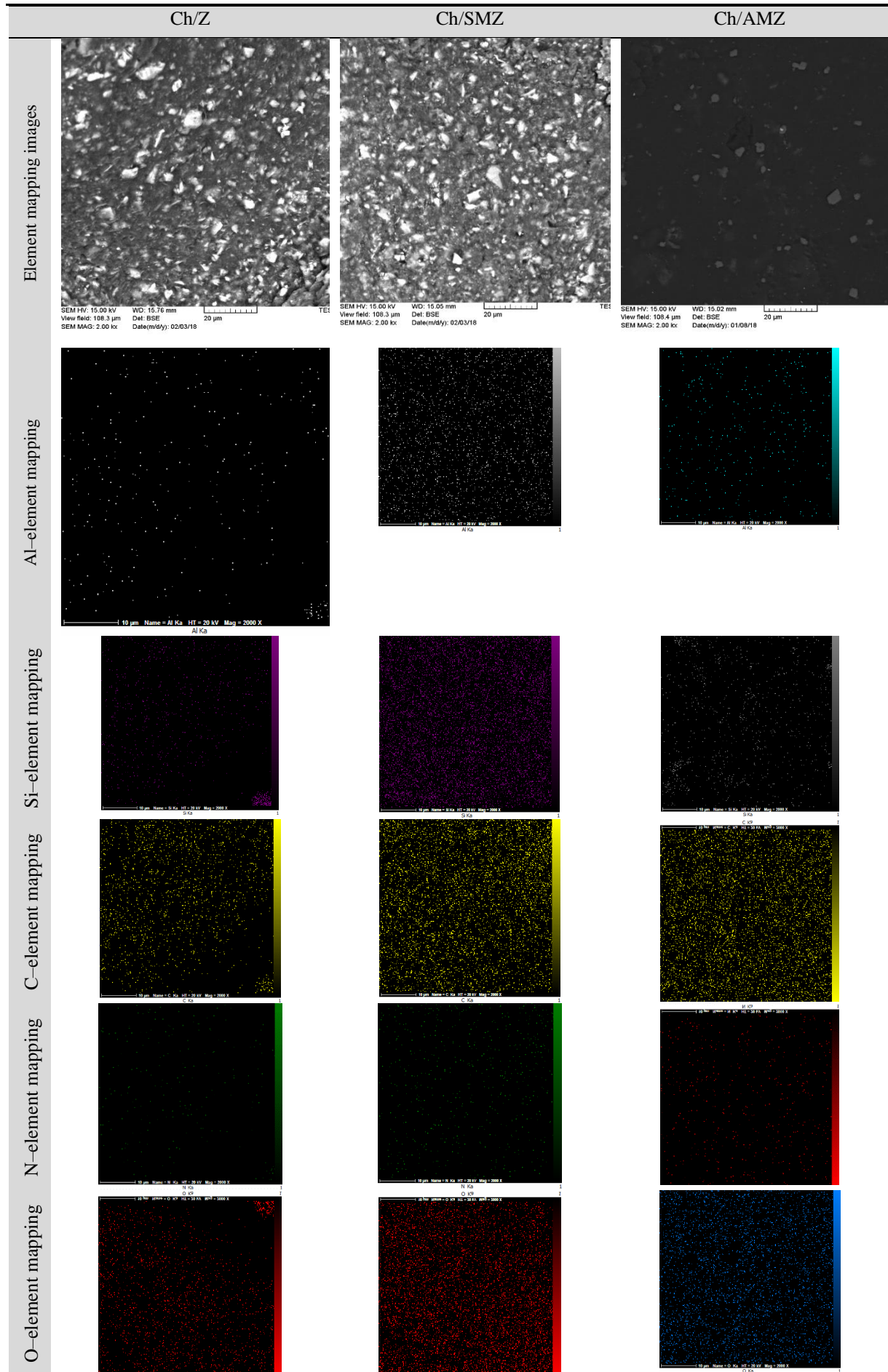Fig. 4. Scanning electron micrographs of (FE-SEM) for Ch/Z, Ch/SMZ, and Ch/AMZ

Fig. 5. Element mapping results for Ch/Z, Ch/SMZ, and Ch/AMZ

Selection of the "Best" Beads

Results of the nitrate removal from aqueous solution using the various beads showed modifications of zeolite increased the removal efficiency (Table 5). When natural zeolite was modified with acid, adsorption of the hydrogen ion on the zeolite structure led to surface protonation. Protonation by acid is the main reason for the dealumination or hydrolysis of the Al–O–Si that causes an increase in the Si/Al ratio and Si–OH groups in the zeolite. Si–OH groups as the hydroxyl groups in zeolite are active sites for hydrogen bonding with nitrate ions, thus, the modification of zeolite by acid led to an increase in the nitrate removal efficiency. When natural zeolite was modified with a surfactant, the surface charge changed from a net negative to a positive charge. Thus, electrostatic forces between the positively charged zeolite and negatively charged nitrate anions caused improved removal efficiency of nitrate. According to the results presented in Table 5, the synthesized Ch/AMZ in this work showed the highest nitrate removal efficiency. Thus, the Ch/AMZ was selected for further nitrate removal studies in the present work.

Table 5. The comparison of the removal nitrate by different beads

Beads	Removal Efficiency (%)
Ch	70.5%
Ch/Z	73.5%
Ch/AMZ	95.0%
Ch/SMZ	88.0%

Response Surface Method (RSM)

The effect of pH, contact time, and bead concentration on the nitrate removal efficiency was investigated by the CCD method. The observed results are presented in Table 6. According to the results of the analysis of variance (ANOVA) using Design-Expert software, the quadratic and linear model was selected as the best model to fit the removal efficiency and adsorption capacity.

Table 6. Central composite design matrix for the experimental design with corresponding results

Trail	pH	Contact Time	Bead Concentration	Removal Efficiency (%)	Adsorption Capacity (mg/g)
1	9.00	40.00	2.00	76.1	19.02
2	5.00	100.00	2.00	83.8	20.95
3	9.00	100.00	2.00	91	22.75
4	7.00	120.45	3.00	99.3	16.48
5	5.00	40.00	2.00	72.88	18.22
6	7.00	70.00	3.00	94.4	15.73
7	7.00	70.00	4.68	98.7	10.55
8	7.00	70.00	3.00	94.9	15.82
9	5.00	100.00	4.00	95.7	11.96
10	7.00	70.00	3.00	98.9	16.55
11	5.00	40.00	4.00	89.9	11.25
12	7.00	70.00	1.32	59.4	22.55
13	7.00	19.55	3.00	82.4	13.73
14	10.36	70.00	3.00	97.8	16.30
15	9.00	100.00	4.00	98.6	12.26
16	3.64	70.00	3.00	95.4	15.90
17	7.00	70.00	3.00	98.7	16.45
18	7.00	70.00	3.00	99.3	16.52
19	7.00	70.00	3.00	99.3	16.47
20	9.00	40.00	4.00	84.1	10.51

In this model for removal efficiency, the coefficient of determination (R^2) is 0.9321 and the value of the adjusted coefficient of determination (R^2_{Adj}) is 0.8709, and for adsorption capacity, R^2 is 0.9883 and R^2_{Adj} is 0.9778. These values show good agreement between the model prediction and the experimental data. As seen from Table 7, C, B^2, and C^2 for removal efficiency and BC and B^2 for adsorption capacity are introduced as important parameters of the model (P-values < 0.0500). According to the regression coefficients for actual factors (positive sign), the removal efficiency increases by increasing the bead concentration, contact time, and pH; these results are similar to what was observed by Yunan Gao et al (2020) for bead concentration and contact time [50]. Also, the high value of pH and the bead concentration coefficients indicated that these parameters have the greatest effect on the removal efficiency.

Table 7. ANOVA of second-order polynomial models for removal efficiency and first-order polynomial models for adsorption capacity

Term	Sum of Squares	df	Mean Square	F-value	P-value	Regression Coefficients for Actual Factors	
Removal Efficiency (%)							
Model	2124.14	9	236.02	15.24	0.0001		Significant
A	19.60	1	19.60	1.27	0.2868	3.527	
B	0.055	1	0.055	0.0036	0.9535	0.491	
C	609.79	1	609.79	39.39	< 0.0001	58.212	
AB	20.10	1	20.10	1.30	0.2811	0.026	
AC	22.18	1	22.18	1.43	0.2590	-0.832	
BC	3.81	1	3.81	0.25	0.6306	-0.023	
A^2	7.10	1	7.10	0.46	0.5136	-0.175	
B^2	107.90	1	107.90	6.97	0.0247	-0.003	
C^2	697.59	1	697.59	45.06	< 0.0001	-7.132	
Constant						-38.977	
Residual	154.83	10	15.48				
Lake of Fit	128.62	5	25.72	4.91	0.0528		Not significant
Pure Error	26.21	5	5.24				
Cor Total	2278.97	19					
Adsorption Capacity							
Term	Sum of Squares	df	Mean Square	F-value	p-value	Regression Coefficients for Actual Factors	
Model	243.44	9	27.05	93.82	< 0.0001		Significant
A	1.01	1	1.01	3.51	0.0905	0.571	
B	1.20	1	1.20	4.17	0.0685	0.116	
C	0.37	1	0.37	1.28	0.2843	-1.94	
AB	0.52	1	0.52	1.79	0.2104	0.004	
AC	1.16	1	1.16	4.01	0.0731	-0.194	
BC	1.99	1	1.99	6.91	0.0252	0.004	
A^2	0.044	1	0.044	0.15	0.7035	-0.017	
B^2	2.38	1	2.38	8.27	0.0165	-0.014	
C^2	0.052	1	0.052	0.18	0.6810	-4.516	
Constant						0.061	
Residual	2.88	10	0.29				
Lake of Fit	2.18	5	0.44	3.11	0.1196		Not significant
Pure Error	0.70	5	0.14				
Cor Total	246.32	19					

In the fitted model for adsorption capacity, the positive sign of the regression coefficients of contact time and pH indicates that adsorption capacity increases by increasing these variables. On the other, adsorption capacity decreases with increasing beads concentration. Also, the value of the coefficients suggested that the bead concentration parameter had the greatest effect on the adsorption capacity.

Table 8 presents several proposed solutions for optimizing the removal efficiency and adsorption capacity in different values of variables by Design Expert software. At the computed optimum operating conditions for removal efficiency (pH = 7.75, 72.60 min contact time, and 3.88 g/L), the maximum nitrate removal efficiency, 98.2% with Ch/AMZ was obtained and 99.3001% was predicted by the software. Also, at the optimum operating condition for adsorption capacity (pH = 4.30, 88.57 min contact time, and 1.33 g/L beads concentration), the maximum adsorption capacity, 22.48 mg/g was obtained and 22.75 mg/g was predicted by the software. The close agreement of the observed and predicted response confirms the accuracy of the proposed model.

Table 8. A number of proposed solutions for optimizing the removal efficiency and adsorption capacity in different values of variables by Design Expert software

	Proposed Solutions for Optimizing the Adsorption Capacity					Proposed Solutions for Optimizing the Removal Efficiency				
	Independent Variables Code			Adsorption Capacity	Desirability	Independent Variables Code			Removal Efficiency	Desirability
No	A	B	C			A	B	C		
1	7.60	73.53	1.54	22.75	1.000	7.75	72.60	3.88	99.3001	1.000
2	7.82	100.30	1.81	22.75	1.000	9.62	100.71	4.11	99.2999	1.000
3	9.99	107.71	2.02	22.75	1.000	4.22	93.87	3.60	99.3000	1.000
4	10.19	67.06	1.63	22.75	1.000	10.18	83.74	2.83	99.3002	1.000
5	9.34	72.13	1.65	22.75	1.000	8.95	71.99	3.68	99.2998	1.000
6	8.26	96.67	1.82	22.75	1.000	8.96	81.47	3.97	99.3000	1.000
7	6.48	85.67	1.57	22.75	1.000	4.30	76.31	3.84	99.2999	1.000
8	5.17	81.22	1.38	22.75	1.000	4.43	82.79	3.95	99.2999	1.000
9	3.95	97.98	1.34	22.75	1.000	7.59	114.69	2.83	99.3002	1.000
10	4.30	88.57	1.33	22.75	1.000	4.86	103.88	3.43	99.2999	1.000

One of the things that should be considered in the design of any absorbent, is the adsorption capacity and removal efficiency of that adsorbent compared to other common adsorbents. The maximum removal efficiency and adsorption capacity obtained here can be compared with the values mentioned in the literature. For removal efficiency, this value is 70.2% of chitosan cross-linked zeolite molecular sieve [50], and 90% of chitosan/polystyrene/zinc [51]. For adsorption capacity, this value is 23.58 for chitosan/zeolite Y/nano ZrO_2 [43], 16.39 for Modified steel slag [52], 14.76 for HTDMA modified bentonite [53] and [51], as reported by other researchers. Therefore, the synthesized adsorbent has a significant adsorption capacity and removal efficiency, compared to another adsorbent.

Figs. 6 & 7 show the interaction between two parameters in the form of response surface 3D plot and contour plot for removal efficiency and adsorption capacity when the other independent variable is kept constant at the median level. Figs. 6a & 6b show the interaction between pH and contact time on the removal efficiency where bead concentration is kept constant at 3 g/L. According to the results, the removal efficiency increases with increasing contact time, but increasing pH does not have a significant effect on the removal efficiency, these results can also be seen in Figs 6c & 6d. Figs. 6e & 6f show that the removal efficiency increases with increasing bead concentration and contact time. At high bead concentration, the reaction efficiency increases with contact time with a very sharp slope. Figs. 7a & 7b show the interaction between the parameters of pH and contact time on the adsorption where bead concentration is kept constant at their median level (3 g/L). This curve shows when the pH is constant, the adsorption capacity increases with increasing contact time and pH. Figs. 7c & 7d show reducing bead concentration increases adsorption capacity and the trend of changes in adsorption capacity with increasing bead concentration is almost the same at different pH. Figs. 7e & 7f show the interaction between contact time and bead concentration on the adsorption capacity. According to the graph, at higher beads concentration, increasing contact time doesn't have a significant effect on the adsorption capacity; however, at low concentrations, increasing contact time increases the adsorption capacity.
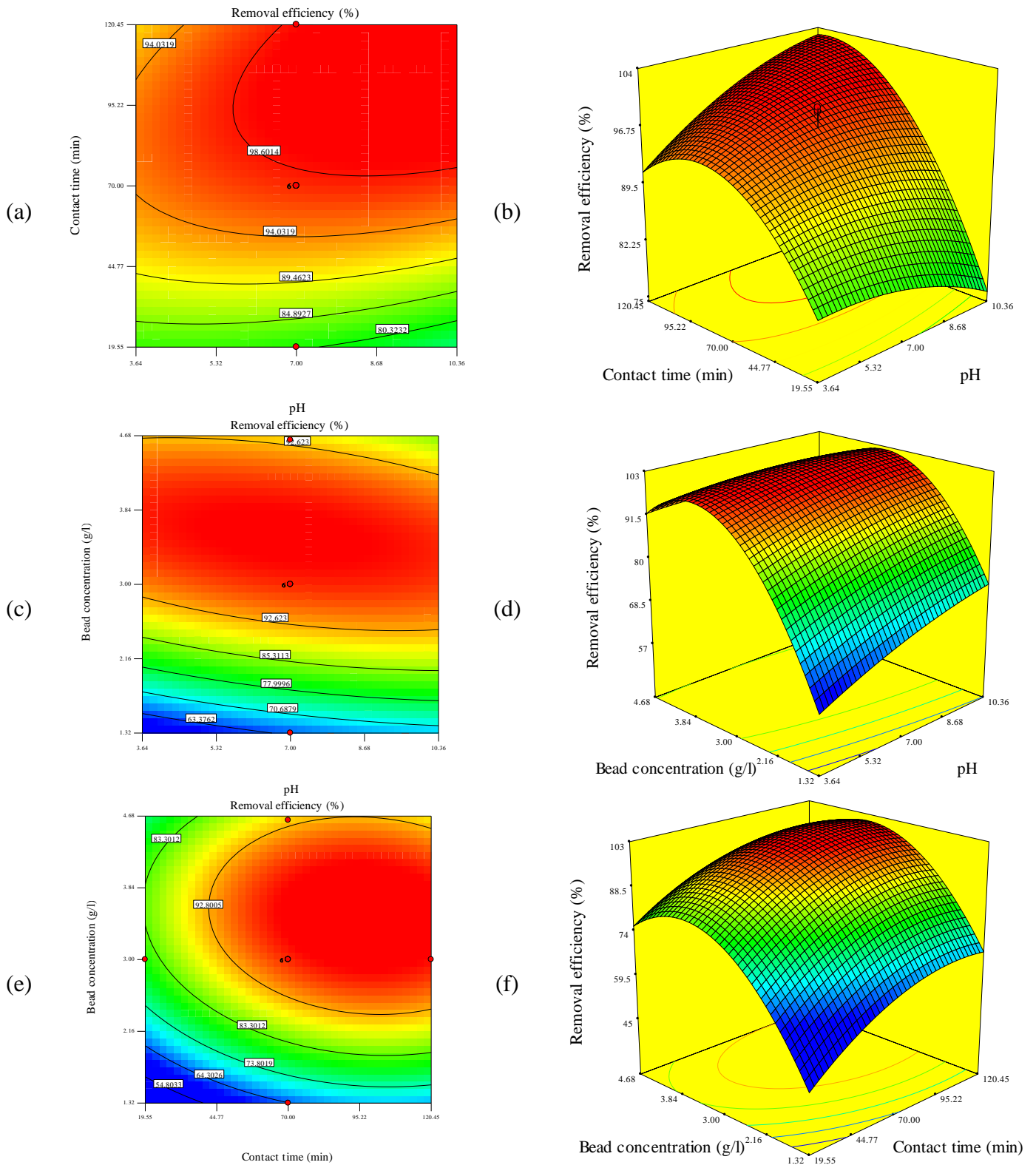
Fig. 6. Response surface 3D plot and contour plot for the interaction of two parameters on the removal efficiency when the other parameters at the middle level
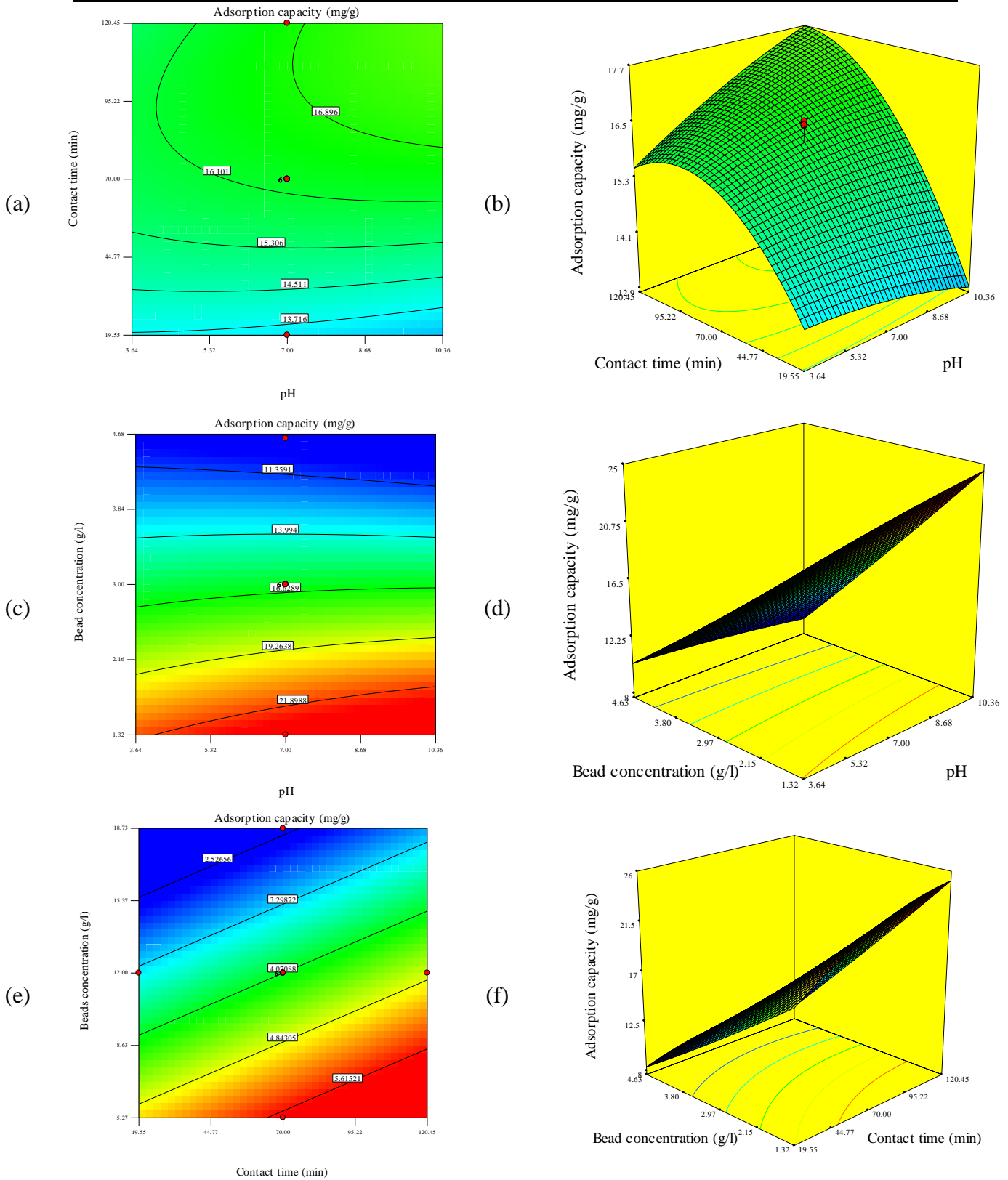
Fig. 7. Response surface 3D plot and contour plot for the interaction of two parameters on adsorption capacity when the other parameters at the middle level

Adsorption Isotherms

Table 9 shows equilibrium concentration and adsorption at different initial concentrations of NO_3-N. Eq. 2 was applied to describe the Linear isotherm:

$$q_e = aC_e + b \tag{2}$$

where *a* and *b* are the Linear constants, C_e denotes the concentration of nitrate in aqueous solution at equilibrium conditions with scale mg/L; q_e means the amount of nitrate adsorbed at equilibrium time (mg/g).

Eq. 3 was applied to describe the Langmuir isotherm:

$$q_e = \frac{q_m b C_e}{[1 + bC_e]} \tag{3}$$

where C_e denotes the concentration of nitrate in aqueous solution at equilibrium conditions with scale mg/L; and q_e means the amount of nitrate adsorbed at equilibrium time (mg/g); q_m is the maximum adsorption capacity of the adsorbent; and *b* is the constant for the binding energy of the adsorption system.

Eq. 4 describes the Freundlich model. K_f and *n* in this equation are Freundlich constants.

$$q_e = K_f C_e^{1/n} \tag{4}$$

The parameters of Linear, Langmuir, and Freundlich models can be determined by regression of the experimental data (Table 9). According to the model parameters and correlation coefficients (R^2) (Table 10), the high value of R^2 of the Freundlich isotherm (0.9732) represents better fitness of this model to the experimental data compared to other models. Table 11 shows a comparative evaluation of the maximum nitrate adsorption capacities for adsorbents reported in previous literature and this work.

Table 9. Variation of equilibrium concentration and adsorption capacity at different initial NO3-N concentration for nitrate adsorption from aqueous solution by Ch/AMZ beads

C_0 (mg/L)	C_e (mg/L)	q_e (mg NO$_3$-N /g beads)
10	0.5	1.7272
25	4	3.8181
40	8	5.8181
65	14	9.2727
80	17	11.4545
100	25	13.6363
120	28	16.7272
150	40	20.0000
180	50	23.6363
200	70	23.6363

Table 10. Model parameters and correlation coefficients (R^2) of Linear, Langmuir and Freundlich isotherms for NO$_3$-N adsorption from aqueous solution by Ch/AMZ beads

Isotherm Model	Equation	Model Parameters		R^2
Linear	$q_e = aC_e + b$	a	0.3426	0.8916
		b	4.4757	
Langmuir	$q_e = \dfrac{q_m b C_e}{[1 + bC_e]}$	q_m	22.026	0.8776
		b	0.0736	
Freundlich	$q_e = K_f C_e^{1/n}$	K_f	2.1607	0.9732
		n	1.71	

Table 11. Comparative evaluation of adsorption capacity of some different adsorbents based on chitosan for nitrate removal

Materials	Initial nitrate Concentration (mg/L)	pH	Dose	T (°C)	Contact Time	Adsorption Capacity (mg/g)	Ref
Chitosan-zeolite (Ch-Z)	3,100	–	0.4 g/250 mL	4	72 h	37.2	[24]
Chitosan-zeolite (Ch-Z)	620	3	0.4 g/250 mL	20	72 h	45.8	[24]
Chitosan/Zeolite/nano ZrO2	20	3	0.02 g/L	35	60 min	42.5	[43]
Surfactant modified Sabzevar zeolite	50	-	15 g/50 mL	30	10 min	0.34	[54]
Chitosan-acid modified Sabzevar zeolite composite beads	200	6	5.5 g/L	25	80 min	23.6363	This work

Conclusion

This study showed that chitosan is successfully mixed with Sabzevar zeolite, acid-modified Sabzevar zeolite, and surfactant-modified Sabzevar zeolite and formed chitosan/zeolite composite beads. The adsorption study showed that chitosan /acid-modified zeolite composite beads could be effectively used to remove nitrate. The adsorption process depends on various parameters, such as pH, contact time, and bead concentration. The optimum operating conditions to reach the maximum removal efficiency and adsorption capacity were determined by RSM design. According to the results, maximum nitrate removal of 97.32% and adsorption capacity of 5.62 mg/g was achieved at optimum operating conditions and the Freundlich isotherm model was superior to the other alternative models for the description of Ch/AMZ adsorption isotherm in the presence of nitrate compounds. In conclusion, the chitosan/Sabzevar zeolite composite beads synthesized in this work can be successfully used as an economical, eco-friendly adsorbent for the removal of nitrate pollution.

Nomenclature

Acid-modified natural zeolite	AMZ
Central composite design	CCD
Chitosan beads	Ch
Chitosan/acid-modified natural zeolite composite beads	Ch/AMZ
Chitosan/ natural zeolite composite beads	Ch/Z
Chitosan/surfactant-modified natural zeolite composite beads	Ch/SMZ
Field Emission Scanning Electron Micrographs	FE-SEM
Fourier-Transform Infrared Spectroscopy	FTIR
Natural zeolite	Z
Response Surface Methodology	RSM
Surfactant modified zeolite	SMZ
Transmission Electron Microscopy	TEM
X-Ray Diffraction	XRD
X-Ray Fluorescence	XRF

Funding

Conflict of Interest:

The authors declare that they have no conflict of interest.

References

[1] Pereira LS. Water, agriculture and food: challenges and issues. Water Resources Management. 2017 Aug;31(10):2985-99. https://link.springer.com/article/10.1007/s11269-017-1664-z

[2] ShenavaeiZare T, Khoshsima A, ZareNezhad B. Development of surfactant-free microemulsion hybrid biofuels employing halophytic salicornia oil/ethanol and oxygenated additives. Fuel. 2021 May 15;292:120249. https://doi.org/10.1016/j.fuel.2021.120249

[3] Sadler R, Maetam B, Edokpolo B, Connell D, Yu J, Stewart D, Park MJ, Gray D, Laksono B. Health risk assessment for exposure to nitrate in drinking water from village wells in Semarang, Indonesia. Environmental pollution. 2016 Sep 1; 216:738-45. https://doi.org/10.1016/j.envpol.2016.06.041

[4] Richards LA, Vuachère M, Schäfer AI. Impact of pH on the removal of fluoride, nitrate and boron by nanofiltration/reverse osmosis. Desalination. 2010 Oct 31;261(3):331-7. https://doi.org/10.1016/j.desal.2010.06.025

[5] Abou-Shady A, Peng C, Bi J, Xu H. Recovery of Pb (II) and removal of NO_3- from aqueous solutions using integrated electrodialysis, electrolysis, and adsorption process. Desalination. 2012 Feb 1;286:304-15. https://doi.org/10.1016/j.desal.2011.11.041

[6] Koparal AS, Öğütveren ÜB. Removal of nitrate from water by electroreduction and electrocoagulation. Journal of hazardous materials. 2002 Jan 4;89(1):83-94. https://doi.org/10.1016/s0304-3894(01)00301-6

[7] Song H, Zhou Y, Li A, Mueller S. Selective removal of nitrate from water by a macroporous strong basic anion exchange resin. Desalination. 2012 Jun 15;296:53-60. https://doi.org/10.1016/j.desal.2012.04.003

[8] Dron J, Dodi A. Comparison of adsorption equilibrium models for the study of $CL-$, NO_3- and $SO42-$ removal from aqueous solutions by an anion exchange resin. Journal of hazardous materials. 2011 Jun 15;190(1-3):300-7. https://doi.org/10.1016/j.jhazmat.2011.03.049

[9] Bhatnagar A, Sillanpää M. A review of emerging adsorbents for nitrate removal from water. Chemical engineering journal. 2011 Apr 1;168(2):493-504. https://doi.org/10.1016/j.cej.2011.01.103

[10] Arbabi M, Golshani N. Removal of copper ions Cu (II) from industrial wastewater: A review of removal methods. Epidemiology and Health System Journal. 2016 Sep 1;3(3):283-93.

[11] Pang Y, Wang J. Various electron donors for biological nitrate removal: A review. Science of the total environment. 2021 Nov 10; 794:148699. https://doi.org/10.1016/j.scitotenv.2021.148699

[12] Rahmani A, Nouri J, KAMAL GS, Mahvi AH, Zare MR. Adsorption of fluoride from water by Al^{3+} and Fe^{3+} pretreated natural Iranian zeolites. https://doi.org/10.22059/ijer.2010.246

[13] Demiral H, Gündüzoğlu G. Removal of nitrate from aqueous solutions by activated carbon prepared from sugar beet bagasse. Bioresource technology. 2010 Mar 1;101(6):1675-80. https://doi.org/10.1016/j.biortech.2009.09.087

[14] Velu M, Balasubramanian B, Velmurugan P, Kamyab H, Ravi AV, Chelliapan S, Lee CT, Palaniyappan J. Fabrication of nanocomposites mediated from aluminium nanoparticles/Moringa oleifera gum activated carbon for effective photocatalytic removal of nitrate and phosphate in aqueous solution. Journal of Cleaner Production. 2021 Jan 25;281:124553. http://dx.doi.org/10.1016/j.jclepro.2020.124553

[15] Cengeloglu Y, Tor A, Ersoz M, Arslan G. Removal of nitrate from aqueous solution by using red mud. Separation and purification technology. 2006 Oct 1;51(3):374-8. https://doi.org/10.1016/j.seppur.2006.02.020

[16] Mishra PC, Patel RK. Use of agricultural waste for the removal of nitrate-nitrogen from aqueous medium. Journal of environmental management. 2009 Jan 1;90(1):519-22. http://dx.doi.org/10.1016/j.jenvman.2007.12.003

[17] Xing X, Gao BY, Zhong QQ, Yue QY, Li Q. Sorption of nitrate onto amine-crosslinked wheat straw: Characteristics, column sorption and desorption properties. Journal of hazardous materials. 2011 Feb 15;186(1):206-11.

[18] Gao BY, Wang Y, Yue QY, Xu X, Yue WW, Xu XM. Adsorption kinetics of nitrate from aqueous solutions onto modified corn residue. International Journal of Environment and Pollution. 2011 Jan 1;45(1-3):58-68. http://dx.doi.org/10.1016/j.colsurfa.2007.05.014

[19] Sharma SK, Sharma MC. Application of Biological Adsorbent Materials for Removal of Harmful Inorganic Contaminants from Aqueous Media–An Overview. Current Trends in Technol Sci. 2015;4:1. https://doi.org/10.1016/j.dwt.2024.100253

[20] Pourbaghaei NZ, Anbia M, Rahimi F. Fabrication of nano zero valent iron/biopolymer composite with antibacterial properties for simultaneous removal of nitrate and humic acid: kinetics and isotherm studies. Journal of Polymers and the Environment. 2022 Mar 1:1-8. http://dx.doi.org/10.21203/rs.3.rs-324935/v1

[21] Dima JB, Sequeiros C, Zaritzky N. Chitosan from marine crustaceans: production, characterization and applications. Biological activities and application of marine polysaccharides. 2017 Jan 11:39-56.

[22] Chatterjee S, Lee DS, Lee MW, Woo SH. Nitrate removal from aqueous solutions by cross-linked chitosan beads conditioned with sodium bisulfate. Journal of hazardous materials. 2009 Jul 15;166(1):508-13. https://doi.org/10.1016/j.jhazmat.2008.11.045

[23] Hu Q, Chen N, Feng C, Hu W. Nitrate adsorption from aqueous solution using granular chitosan-Fe3+ complex. Applied surface science. 2015 Aug 30;347:1-9. http://dx.doi.org/10.1016/j.apsusc.2015.04.049

[24] Arora M, Eddy NK, Mumford KA, Baba Y, Perera JM, Stevens GW. Surface modification of natural zeolite by chitosan and its use for nitrate removal in cold regions. Cold Regions Science and Technology. 2010 Jul 1;62(2-3):92-7. https://doi.org/10.1016/j.coldregions.2010.03.002

[25] Chatterjee S, Woo SH. The removal of nitrate from aqueous solutions by chitosan hydrogel beads. Journal of hazardous materials. 2009 May 30;164(2-3):1012-8. https://doi.org/10.1016/j.jhazmat.2008.09.001

[26] Jing MI, Lingling LI, Guohua CH, Congjie GA, Shengxiong DO. Preparation of N, O-carboxymethyl chitosan composite nanofiltration membrane and its rejection performance for the fermentation effluent from a wine factory. Chinese Journal of Chemical Engineering. 2008 Apr 1;16(2):209-13. https://doi.org/10.1016/S1004-9541(08)60064-6

[27] Huang R, Liu Q, Zhang L, Yang B. Utilization of cross-linked chitosan/bentonite composite in the removal of methyl orange from aqueous solution. Water Science and Technology. 2015 Jan 1;71(2):174-82. https://doi.org/10.2166/wst.2014.478

[28] Cheng H, Zhu Q, Wang A, Weng M, Xing Z. Composite of chitosan and bentonite cladding Fe–Al bimetal: Effective removal of nitrate and by-products from wastewater. Environmental Research. 2020 May 1; 184:109336. https://doi.org/10.1016/j.envres.2020.109336

[29] An JH, Dultz S. Adsorption of tannic acid on chitosan-montmorillonite as a function of pH and surface charge properties. Applied Clay Science. 2007 May 1;36(4):256-64. https://doi.org/10.1016/j.clay.2006.11.001

[30] Jintakosol T, Nitayaphat W. Adsorption of silver (I) from aqueous solution using chitosan/montmorillonite composite beads. Materials research. 2016 Aug 22;19(5):1114-21. http://dx.doi.org/10.1590/1980-5373-MR-2015-0738

[31]   Deng Z, Zhen Z, Hu X, Wu S, Xu Z, Chu PK. Hollow chitosan–silica nanospheres as pH-sensitive targeted delivery carriers in breast cancer therapy. Biomaterials. 2011 Jul 1;32(21):4976-86. http://dx.doi.org/10.1590/1980-5373-MR-2015-0738

[32]   Liu YL, Wu YH, Tsai WB, Tsai CC, Chen WS, Wu CS. Core–shell silica@ chitosan nanoparticles and hollow chitosan nanospheres using silica nanoparticles as templates: preparation and ultrasound bubble application. Carbohydrate polymers. 2011 Mar 1;84(2):770-4. http://dx.doi.org/10.1016/j.carbpol.2010.03.033

[33]   Metin AÜ, Alver E. Fibrous polymer-grafted chitosan/clay composite beads as a carrier for immobilization of papain and its usability for mercury elimination. Bioprocess and biosystems engineering. 2016 Jul;39:1137-49. https://doi.org/10.1007/s00449-016-1590-0

[34]   Dinçer A, Becerik S, Aydemir T. Immobilization of tyrosinase on chitosan–clay composite beads. International Journal of Biological Macromolecules. 2012 Apr 1;50(3):815-20. https://doi.org/10.1016/j.ijbiomac.2011.11.020

[35]   Golie WM, Upadhyayula S. Continuous fixed-bed column study for the removal of nitrate from water using chitosan/alumina composite. Journal of Water Process Engineering. 2016 Aug 1;12:58-65. https://doi.org/10.1016/j.jwpe.2016.06.007

[36]   Hasan S, Ghosh TK, Viswanath DS, Boddu VM. Dispersion of chitosan on perlite for enhancement of copper (II) adsorption capacity. Journal of Hazardous Materials. 2008 Apr 1;152(2):826-37. https://doi.org/10.1016/j.jhazmat.2007.07.078

[37]   Javanbakht V, Ghoreishi SM, Habibi N, Javanbakht M. A novel magnetic chitosan/clinoptilolite/magnetite nanocomposite for highly efficient removal of Pb (II) ions from aqueous solution. Powder Technology. 2016 Nov 1;302:372-83. https://doi.org/10.1016/j.ijbiomac.2023.125984

[38]   Djelad A, Morsli A, Robitzer M, Bengueddach A, Di Renzo F, Quignard F. Sorption of Cu (II) ions on chitosan-zeolite X composites: Impact of gelling and drying conditions. Molecules. 2016 Jan 19;21(1):109. https://doi.org/10.3390/molecules21010109

[39]   Yang K, Zhang X, Chao C, Zhang B, Liu J. In-situ preparation of NaA zeolite/chitosan porous hybrid beads for removal of ammonium from aqueous solution. Carbohydrate polymers. 2014 Jul 17;107:103-9. https://doi.org/10.1016/j.carbpol.2014.02.001

[40]   Lin J, Zhan Y. Adsorption of humic acid from aqueous solution onto unmodified and surfactant-modified chitosan/zeolite composites. Chemical engineering journal. 2012 Aug 15;200:202-13. https://doi.org/10.1016/j.cej.2012.06.039

[41]   Zhao Y, Zhao X, Deng J, He C. Utilization of chitosan–clinoptilolite composite for the removal of radiocobalt from aqueous solution: Kinetics and thermodynamics. Journal of Radioanalytical and Nuclear Chemistry. 2016 May;308:701-9. http://dx.doi.org/10.1007/s10967-011-1352-z

[42]   Safie NN, Zahrim AY. Recovery of nutrients from sewage using zeolite-chitosan-biochar adsorbent: current practices and perspectives. Journal of Water Process Engineering. 2021 Apr 1;40:101845. https://doi.org/10.1016/j.jwpe.2020.101845

[43]   Teimouri A, Nasab SG, Vahdatpoor N, Habibollahi S, Salavati H, Chermahini AN. Chitosan/Zeolite Y/Nano ZrO2 nanocomposite as an adsorbent for the removal of nitrate from the aqueous solution. International journal of biological macromolecules. 2016 Dec 1;93:254-66. https://doi.org/10.1016/j.ijbiomac.2016.05.089

[44]   Gao Y, Ru Y, Zhou L, Wang X, Wang J. Preparation and characterization of chitosan-zeolite molecular sieve composite for ammonia and nitrate removal. Advanced Composites Letters. 2018 Sep;27(5):096369351802700502. http://dx.doi.org/10.1177/096369351802700502

[45]   Mokhtari-Hosseini ZB, Kazemiyan E, Tayebee R, Shenavaei-Zare T. Optimization of ammonia removal by natural zeolite from aqueous solution using response surface methodology. Hemijska industrija. 2016;70(1):21-9. http://dx.doi.org/10.2298/HEMIND141007006M

[46] Azari A, MAHVI AH, Naseri S, REZAEI KR, Saberi M. Nitrate removal from aqueous solution by using modified clinoptilolite zeolite.

[47] Malekian R, Abedi-Koupai J, Eslamian SS. Use of zeolite and surfactant modified zeolite as ion exchangers to control nitrate leaching. International Journal of Geological and Environmental Engineering. 2011 Apr 23;5(4):267-71.

[48] ShenavaeiZare T, Khoshsima A, ZareNezhad B. Production of biodiesel through nanocatalytic transesterification of extracted oils from halophytic safflower and salicornia plants in the presence of deep eutectic solvents. Fuel. 2021 Oct 15;302:121171. http://dx.doi.org/10.1016/j.fuel.2021.121171

[49] Hu X, Cheng Z. Removal of diclofenac from aqueous solution with multi-walled carbon nanotubes modified by nitric acid. Chinese journal of chemical engineering. 2015 Sep 1;23(9):1551-6. https://doi.org/10.1016/j.cjche.2015.06.010

[50] Gao Y, Bao S, Zhang L, Zhang L. Nitrate removal by using chitosan/zeolite molecular sieves composite at low temperature: Characterization, mechanism, and regeneration studies. Desalin Water Treat. 2020 Nov 1;203:160-71. https://doi.org/10.5004/dwt.2020.26219

[51] Keshvardoostchokami, M., et al., Nitrate removal from aqueous solutions by ZnO nanoparticles and chitosan-polystyrene–Zn nanocomposite: Kinetic, isotherm, batch and fixed-bed studies. International journal of biological macromolecules, 2017. 101: p. 922-930. https://doi.org/10.1016/j.ijbiomac.2017.03.162

[52] Yang LiYun YL, Yang MaoMao YM, Xu Ping XP, Zhao XianCong ZX, Bai Hao BH, Li Hong LH. Characteristics of nitrate removal from aqueous solution by modified steel slag. https://doi.org/10.3390/w9100757

[53] Xi Y, Mallavarapu M, Naidu R. Preparation, characterization of surfactants modified clay minerals and nitrate adsorption. Applied Clay Science. 2010 Mar 1;48(1-2):92-6. https://doi.org/10.1016/j.clay.2009.11.047

[54] Mokhtari-Hosseini ZB, Bikhabar GR, Shenavaei Zare T. Nitrate removal from aqueous solution: Screening of variables and optimization. Advances in Environmental Technology. 2023 Jan 1;9(1):73-83. https://doi.org/10.22104/aet.2023.5653.1596